Proc. Natl. Acad. Sci. USA
Vol. 95, pp. 10251–10256, August 1998
Neurobiology

Synaptic signaling in an active central network only moderately changes passive membrane properties

MORTEN RAASTAD*, MANUEL ENRÍQUEZ-DENTON, AND OLE KIEHN

Section of Neurophysiology, Department of Physiology, The Panum Institute, Blegdamsvej 3, 2200 Copenhagen N, Denmark

Communicated by Per. O. Andersen, University of Oslo, Oslo, Norway, June 26, 1998 (received for review May 20, 1997)

ABSTRACT **The membrane resistance of mammalian central neurons may be dramatically reduced by synaptic events during network activity, thereby changing their integration properties. We have used the isolated neonatal rat spinal cord to provide measurements of the effect of synaptic signaling on passive membrane properties during network activity. Synaptic signaling could take place during fictive locomotor activity with only modest (on average 35%) reduction of the input resistance (R_{in}) and of the cell's charging time constant (τ_{in}). Individual synaptic signals, however, often introduced a peak conductance that was greater than the input conductance ($G_{in} = 1/R_{in}$) without synaptic activity. The combination of moderate average synaptic conductance and large conductance of individual synaptic signals suggests that individual presynaptic neurons have large but short-lasting influence on the integration properties of postsynaptic neurons.**

With the development of the patch clamp technique for intracellular recording from neurons (1, 2) it became obvious that nerve cells could have much higher values for input resistance (R_{in}) and charging time constant (τ_{in}) than had been reported in studies using sharp microelectrodes (3, 4). The values of R_{in} and τ_{in} are important because they influence how neurons integrate the information they receive through synaptic currents. Both these integration parameters depend on the membrane resistance. An important question is, therefore, whether high values for R_{in} and τ_{in} are maintained when cells are bombarded by synaptic signals during network activity. The synaptic conductances will obviously reduce R_{in} and τ_{in}, but the magnitude of this reduction is unknown. Theoretical studies have suggested that synaptic activity may decrease the specific membrane resistance (R_m) in pyramidal cells by a factor of 10 (5), and therefore change their integration properties fundamentally (6). To test this hypothesis, we compared both τ_{in} and R_{in} with and without synaptic network activity.

We used the isolated spinal cord from neonatal rats, which under the influence of certain neuroactive compounds produces a locomotor-like rhythmic activity that can be monitored as bursts of action potentials in the ventral roots (7–11). The activity level of the network is sufficient to maintain a rhythmic pattern similar to that seen in intact animals, with alternation between flexors and extensors, between left and right side, and with a sequential activation of appropriate muscle groups (11). Because this activity resembles the activity seen in intact animals, the preparation is well suited for studies of neuronal network activity. The interneurons can be recorded from with low-resistance patch electrodes (12), allowing good resolution of the fast synaptic signals and the opportunity to reduce the effect of active membrane properties by voltage clamping the soma. We recorded from interneurons in laminae VII and X of the lumbar spinal cord because these areas are particularly active during fictive locomotion (13, 14) and most neurons here are rhythmically modulated (12). These areas also seem to harbor essential elements of the network generating the rhythm (15, 16).

METHODS

Preparation. The preparation has previously been described in detail (7, 8, 12). Briefly, neonatal rats 0–3 days old were deeply anesthetized with ether, decapitated, and eviscerated. The spinal cord extending from the C1 to L6, including ventral and dorsal roots, was isolated. For better electrode access, the dorsal part of the spinal cord was removed from directly above the recording sites. This manipulation does not reduce the amplitude or frequency of the root activity (15). The preparation was transferred to a recording chamber and superfused with oxygenated (95% O_2 and 5% CO_2) Ringer's solution of the following composition (in mM): 128 NaCl, 4.7 KCl, 1.2 KH_2PO_4, 1.25 $MgSO_4$, 2.5 $CaCl_2$, and 20 glucose (pH 7.4). The experiments were performed at room temperature.

Induction of Rhythmic Activity. Locomotion was induced by bath application of *N*-methyl-D-aspartic acid (NMDA; 5–9 μM) in combination with 5-hydroxytryptamine (5-HT; 5–40 μM). A description of the locomotor rhythm induced by these drugs can be found in refs. 10, 12, and 17. After testing the membrane properties during synaptic activity, tetrodotoxin (TTX; 1 μM) was added to the superfusion fluid while NMDA and 5-HT were still present. It took 2–3 hr to wash out 1 μM TTX, which made it difficult to reestablish the conditions that were present before TTX block while recording from the same cell.

Recordings. The L2 and L5 ventral root activities, corresponding to flexor and extensor activity, respectively (11), were recorded with suction electrodes. Interneurons were recorded from with patch electrodes pulled to a final resistance of 5–10 MΩ. The access resistance was usually below 30 MΩ. Whole-cell voltage or current clamp recordings were performed with an Axopatch 1-D amplifier. Because this amplifier may give erroneous voltage measurements in current clamp mode (18), we measured the resistance in both voltage and current clamp mode, with similar results.

The signals were low-pass filtered at 2–5 kHz and digitized at 5 kHz. The pipette solution contained, in mM: 128 potassium gluconate, 10 Hepes, 4 NaCl, 10 CsCl, 0.0001 $CaCl_2$, 4 MgATP, 0.3 LiGTP. The pH was adjusted to 7.3 with KOH. Intracellular potentials were not corrected for liquid junction potentials in the whole-cell configuration (19).

Measurements of τ_{in} and R_{in}. τ_{in} and R_{in} were estimated in current clamp by fitting functions to the cell's voltage responses to rectangular current pulses, 300 ms in duration. The func-

The publication costs of this article were defrayed in part by page charge payment. This article must therefore be hereby marked "*advertisement*" in accordance with 18 U.S.C. §1734 solely to indicate this fact.

Abbreviations: NMDA, *N*-methyl-D-aspartic acid; 5-HT, 5-hydroxytryptamine; TTX, tetrodotoxin; PSC, postsynaptic current; PSP, postsynaptic potential; PSG, postsynaptic conductance.

*To whom reprint requests should be addressed at: Inst. for Basic Medical Sciences, Dept. of Neurophysiology, University of Oslo, Box 1104, 0317 Oslo, Norway. e-mail: mortenra@basalmed.uio.no.

tions included a baseline as long as the fitted test pulse to average out baseline fluctuations resulting from the ongoing synaptic activity. The functions were fitted by minimizing the squared deviation between the function and the data between 5 and 25 ms after the onset of the pulse. This interval was chosen to avoid both the initial period where charge still is redistributing along the dendritic axis (20) and the late intervals with poor signal-to-noise ratio. Simulations with dendrites of plausible lengths (see *Discussion*) showed that the measured time constant (τ_{in}) fitted over the time range 5–25 ms was close to the real membrane time constant (τ_m). The function used was: $f(t) = V_{ss} - \{V_{ss} \cdot \exp(t/\tau_{in})\}$, where V_{ss} is the steady state response. $R_{in} = V_{ss}/I$, where I was -10 or -20 pA when the cell was kept at -45 mV and ± 10 or ± 20 pA when the cell was kept at -65 mV. The influence of changes in the membrane resistance (R_m) on these parameters is explored in a simulation described in *Discussion*. The electrode capacitance was compensated electronically in the cell-attached mode before breaking the seal. For the voltage clamp responses we calculated R_{in} as the command step size divided by the steady-state current response. The access resistance was estimated in voltage clamp as the voltage step divided by the initial current peak in the current response. The access resistance was not compensated electronically in current clamp, and was therefore estimated off-line as the instantaneous pure resistive component in the voltage response divided by the current step. R_{in} was then corrected by subtracting the access resistance.

Algorithm to Detect Synaptic Events. We used a computer algorithm to detect postsynaptic currents (PSCs) followed by visual inspection of the PSCs to control that they had a shape as expected for PSCs. The algorithm estimated the differences between three equally spaced time points, *a*, *b*, and *c*. Each point was the average of 1 ms and separated by 2 or 3 ms. A PSC was detected if the absolute value of the difference between *b* and *c* was above a certain threshold, indicating a steep line for the start of the PSC, while the absolute difference between *a* and *b* was less than 1/10 of the same threshold, indicating a relatively flat baseline before the PSC. The threshold was set in an interactive procedure so that the accepted events had shapes as expected of PSCs, with an abrupt start, fast rise time, and slower decay.

RESULTS

Effect of Synaptic Activity on τ_{in} and R_{in} over Time. Rhythmic locomotor-like activity was induced by adding NMDA in combination with 5-HT to the bath. The motoneuron activity was recorded from the ventral roots (Fig. 1*A*, lower trace), while rhythmic synaptic information from the locomotor network was seen in interneurons as fluctuations of the membrane potential in correlation with motoneuron spike activity (Fig. *1A*, upper trace). The cell was first kept at -45 mV, close to the threshold for spike generation and postsynaptic potentials (PSPs) can be seen as depolarizing and hyperpolarizing events (Fig. *1A*, upper trace). Each PSP is due to a short-lasting increase of the membrane conductance which is added to the total membrane conductance and, therefore, theoretically reduces τ_{in} and R_{in}.

In the following calculations we distinguish between the conductance underlying these individual synaptic signals and the average synaptic conductance over time (avG_{syn}). To estimate the effects of avG_{syn} on τ_{in} and R_{in} we averaged voltage responses to 300-ms current pulses (at least 25) injected through the electrode with and without synaptic activity. These pulses were considerably longer than the duration of the individual synaptic events and not correlated with the rhythmic synaptic activity. The estimates, therefore, give an average estimate of the integration properties of the cell. Assuming that voltage-sensitive conductances are not activated by the synaptic currents (see later), the avG_{syn} will obey the same rules as other membrane conductances, and can therefore be treated as a part of the total membrane conductance.

Fig. 1*A1* shows the averaged initial charging of the membrane in response to 25 hyperpolarizing current pulses (-20 pA, 200 ms) injected during rhythmic activity. The SEM is shown as a dotted line. The dominating time constant (τ_{in}), measured by fitting an exponential function (see *Methods*), was 65 ms. When all presynaptic activity was abolished by bath

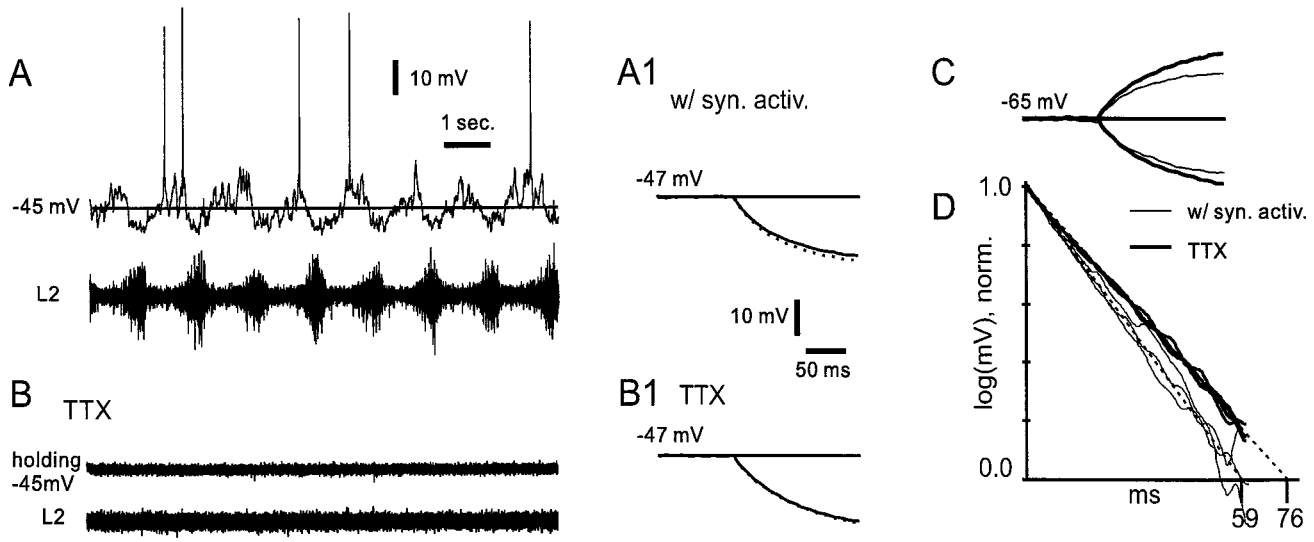

FIG. 1. Impact of locomotor-related synaptic signaling on τ_{in}. (*A*) Intracellular tight-seal voltage recording (upper trace) from a rhythmically active interneuron in the isolated neonatal rat spinal cord during 5-HT- and NMDA-induced locomotor-related activity. No holding current was applied. The motoneuron activity was recorded from the ventral roots (lower trace). (*A1*) With the neuron hyperpolarized just below spike threshold, the charging time constant (τ_{in}), measured from the average of the voltage response to 25 hyperpolarizing current steps (-20 pA), was 65 ms. SEM is added as a dotted line. (*B*) Seven minutes after bath application of TTX, the synaptic currents and the root activity disappeared. (*B1*) The average τ_{in} of the voltage response was now 80 ms (same size current injection). (*C*) With the cell hyperpolarized to -65 mV the voltage responses to depolarizing and hyperpolarizing current steps (± 20 pA) showed τ_{in} of 56 and 58 ms before (thin lines) and 76 and 73 ms after (thick lines) TTX application. (*D*) τ_{in} of the voltage responses in *A1*, *B1*, and *C* can be better evaluated as the negative slope on a semilogarithmic plot. Thin lines before and thick lines after TTX application.

application of TTX (but with NMDA and 5-HT still in the bath) the PSPs disappeared, as did all spike activity in the ventral root (Fig. *1B*). The time constant then measured 81 ms (Fig. 1*B1*), 25% longer than τ_{in} during synaptic activity. R_{in} measured as the amplitude of the injected current divided by the steady-state voltage response (outside the end of the trace), increased from 0.70 to 0.90 GΩ, or 29%, in response to TTX application.

The increases in τ_{in} and R_{in} are probably due to an increase in the membrane resistance (R_m), because the synaptic conductance (and possibly TTX-sensitive) conductances disappeared. One assumption for this conclusion is that voltage-activated currents did not interfere with the measurements. For example, some membrane currents that were active around −45 mV may have been deactivated at the more hyperpolarized levels induced by the test pulse. Furthermore, some of these presumed voltage-dependent effects may have been abolished by the addition of TTX. Therefore we repeated the test with the cell held at −65 mV, and we used both depolarizing and hyperpolarizing current pulses to control for rectification of the membrane (Fig. 1*C*). The two thick curves are the responses with TTX in the bath. During rhythmic activity τ_{in} was 56 and 58 ms for depolarizing and hyperpolarizing pulses, respectively. In TTX the same parameters increased to 76 and 73 ms. These changes are in the same range as the estimates obtained at −45 mV. The differences between τ_{in} at both membrane potentials and for both hyperpolarizing and depolarizing pulses are better seen in a semilogarithmic plot (Fig. 1*D*), where the thin and thick lines are the responses with and without synaptic activity, respectively. The similarity within these two groups of three measurements suggests that voltage-sensitive conductances probably did not interfere significantly with the estimates of τ_{in} in this cell.

We measured τ_{in} in 20 cells and R_{in} in 27 cells from 25 different preparations while there was rhythmic activity in the ventral roots, and when all activity was blocked by TTX. In all cells, the network activity was seen as rich synaptic activity (see Fig. 1*A*), and 20 of 27 analyzed cells were rhythmically modulated. Fig. 2*A* (*Upper*) shows τ_{in} measured at a depolarized membrane potential by using hyperpolarizing pulses (DH), and at a hyperpolarized membrane potential by using both depolarizing (HD) and hyperpolarizing (HH) pulses, before (open bars) and during TTX blockade (filled bars). Each bar gives the average of all cells, based on measurements of at least 25 pulses in each test. Fig. 2*B* (*Upper*) shows the estimates for R_{in}, and here the estimates were also made in voltage clamp. The range for τ_{in} was 12–84 ms, and for R_{in} 0.18–1.6 GΩ. The expected increases in τ_{in} and R_{in} in response to blocking the synaptic activity with TTX were too small to be significant ($P > 0.05$, one-way repeated measures MANOVA). The SEM, added as vertical lines on top of the bars, does not give large confidence intervals. The SEM constitutes less than 10% of all the average τ_{in} and R_{in} values. There were also no significant differences between the tests, supporting the theory that voltage-sensitive conductances did not interfere significantly with the estimates. The average relative change in τ_{in} and R_{in} is shown in the lower part of Fig. 2 *A* and *B*. These relative changes showed no significant differences either, suggesting that blocking synaptic network activity gave only small changes of τ_{in} and R_{in}.

In some cells we observed a steady change, usually a reduction, of τ_{in} and R_{in} during the recording period. This is obscured in the estimates for the entire recording period before and after TTX application (Fig. 2 *A* and *B*). To estimate the error introduced by this change, we divided the duration of the recording (20–40 min) into five equal time intervals, three before and two after TTX application. The values for τ_{in} and R_{in} were then normalized with respect to their average value in the first three time bins. The average spontaneous change of τ_{in} and R_{in} in the individual cells was calculated as the average change between bin 1 and 2, 2 and 3, and 4 and 5. The average change was a decline of 9% for τ_{in} (range −42% to

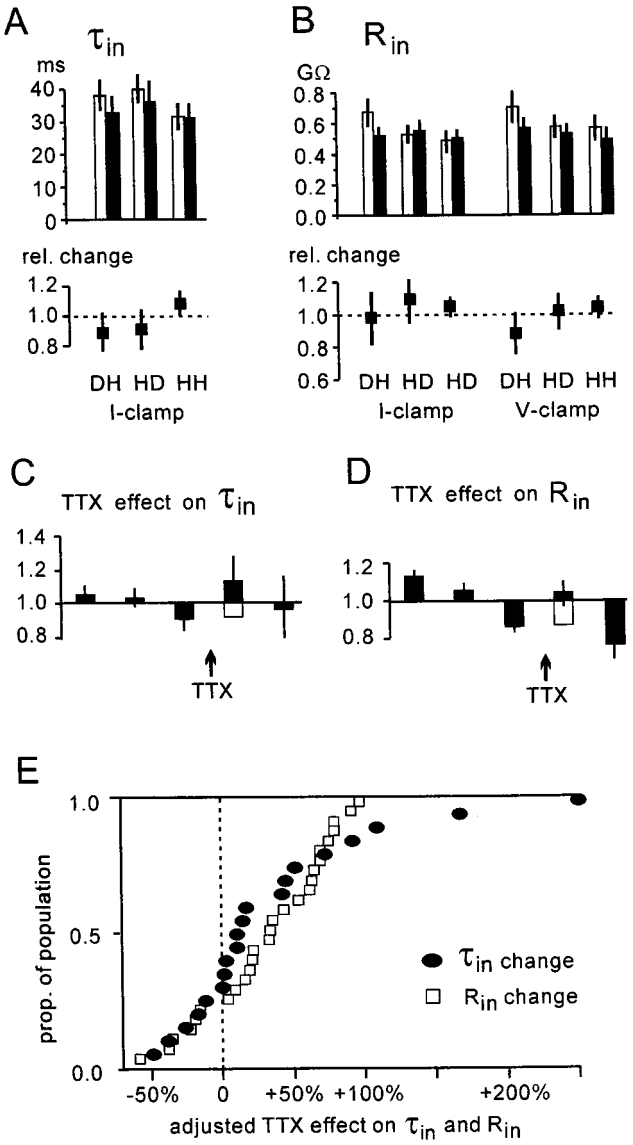

FIG. 2. Estimates of τ_{in} and R_{in} with and without network activity. (*A*) τ_{in} was measured with network activity (open bars) and with all activity blocked by TTX (filled bars) at depolarized holding potential with hyperpolarizing steps (DH), and at hyperpolarized potentials with both depolarizing steps (HD) and hyperpolarizing steps (HH). The SEM (20 cells) is given as vertical lines on top of the bars. τ_{in} was not significantly different comparing the tests before and after TTX, or comparing the different tests (one-way repeated measures MANOVA, $P > 0.05$). (*B*) The mean R_{in} with and without presynaptic activity, and the relative changes (*Lower*) did not show significant differences when the same test as in A was used. For R_{in}, voltage clamp was also used for the measurements (right three groups). (*C*) The estimates from the individual cells were divided in three parts of equal duration before TTX application, and two equal parts after TTX. The values for τ_{in} were normalized to the average value in the first three bins. The averages of the τ_{in}, measured in the resulting five time bins in all 20 cells, are given as five bars, with the SEM added as a vertical line. If we assume that the declining tendency seen between the first three bins continued also during TTX application, we can add a new base (open bar) for the increase induced by TTX. Including this correction, τ_{in} increased on average 35% (open plus filled bar). (*D*) The average increase in R_{in}, calculated in the same way as explained for τ_{in} in *C*, was also 35% after addition of the extrapolated decline (open plus filled bar). (*E*) Effect of blocking network activity with TTX, adjusted for the expected decline in R_{in}, calculated for the individual cells (τ_{in} calculated in 20 cells and R_{in} in an additional 7).

+25%), and 17% for R_{in} (range −50% to +13%). This spontaneous change was probably present also between time bins 3 and 4, when TTX was applied, causing an underestimate for changes in τ_{in} and R_{in}. Therefore we added this expected change (open bars in Fig. 2 *C* and *D*) to the change induced by TTX, giving an adjusted total average increase in both τ_{in} and R_{in} of 35%.

Fig. 2*E* shows the cumulative distribution for τ_{in} in 20 cells and R_{in} in 27 cells, adjusted as described for the spontaneous change in the individual cells. In response to block of synaptic activity, τ_{in} (filled circles) increased between 5% and 280% in 15 of 20 cells and R_{in} increased between 5% and 127% in 21 of 27 cells. There was a reduction of τ_{in} in 5 cells and of R_{in} in 6 cells, probably reflecting statistical uncertainty and the fact that the currents measured were very small.

Reduction of R_{in} by Individual PSCs. So far, all conductances have been calculated as averages over a duration much longer than the duration of individual synaptic events. Because R_{in} increased on average 35% and in no case more than 100%, the average synaptic conductance (avG_{syn}) was smaller than the input conductance ($G_{in} = 1/R_{in}$) without synaptic activity. However, the membrane current, and therefore the conductance, was far from homogeneous over time. Fig. 3*A* shows the current recorded in the same cell as used in Fig. 1, during 8 s of locomotor-related activity. The current is characterized by large-amplitude transient events, probably PSCs.

In Fig. 3*B* we compare the underlying conductance of these PSCs with G_{in} with and without synaptic activity. G_{in} is illustrated in voltage clamp by dividing the current responses (average of 15 responses) by the step command (−10 mV). The hatched area represents the part of the input conductance that disappeared in response to TTX application. In the same cell PSCs were identified with a detection algorithm. The PSCs were converted into conductances assuming a reversal potential for excitatory PSCs (EPSCs) at 0 mV and a reversal potential for inhibitory PSCs (IPSCs) at −53 mV (measured in 55 cells with 10 mM Cl^- in the pipette). The *Inset* of Fig. 3*B* shows 10 IPSCs and 10 EPSCs converted into conductances (IPSGs and EPSGs, respectively).

Some of the larger PSCs had a peak conductance that was as big as G_{in} (the steady-state part of the charging curves). Fig. 3*C* shows the distribution of the peak conductances of the EPSGs and IPSGs (filled and open bars, respectively) detected in one cell. The peak conductance is probably even larger at the synapse because the fast currents were filtered by the dendritic cable when arriving at soma. The values reflect, however, the conductance change that will affect the integration properties of the somatic compartment. Below the *x*-axis is also marked G_{in} without synaptic activity and the average synaptic conductance (avG_{syn}). Many individual synaptic signals gave a contribution to the input conductance that was considerably larger than the basal value. We repeated these estimates in 14 cells (14 preparations) with a good signal-to-noise ratio. All these cells showed similarly skewed distributions of synaptic conductances with many small but some large conductances that were greater than the basic G_{in} present without synaptic activity. The large conductance from a few synaptic signals probably gave a membrane conductance that was very heterogeneous over time.

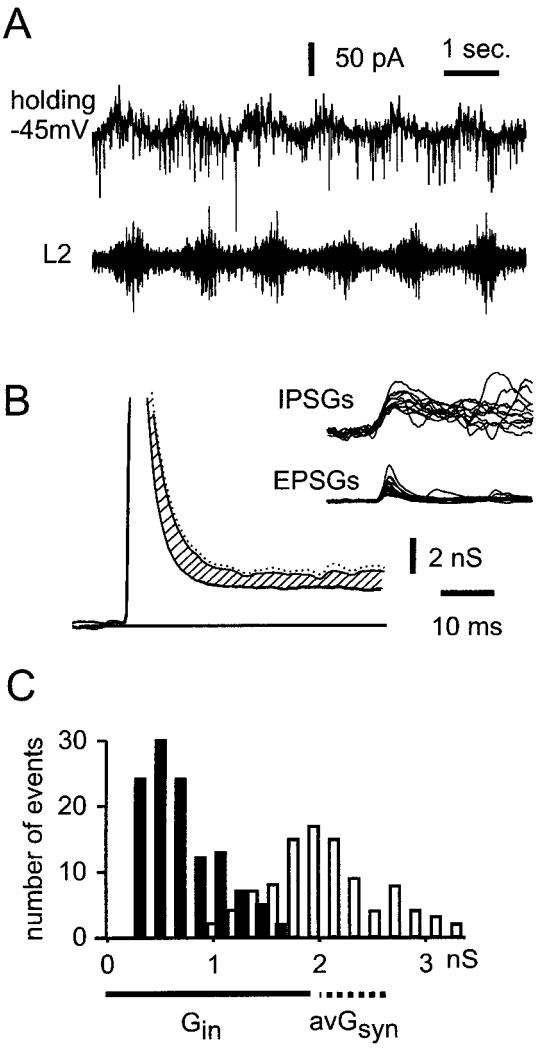

FIG. 3. Contribution from individual PSCs to G_{in}. (*A*) During rhythmic activity in the ventral root (L2, lower trace), the membrane current (upper trace) consists of fast events, presumably PSCs, in positive and negative direction on a modestly fluctuating baseline. (*B*) The current in response to a 10-mV step in the command potential was converted to the corresponding conductance by dividing it by the driving voltage (10 mV). The upper curve gives the conductance with synaptic activity (dotted line gives SEM), and the lower gives the conductance after TTX application. The hatched area gives avG_{syn}. *Inset* shows 10 excitatory PSCs (EPSCs) and 10 inhibitory PSCs (IPSCs), also converted into conductances (EPSGs and IPSGs). The largest PSGs were of the same magnitude as the basal G_{in} without synaptic activity. (*C*) Distribution of amplitudes of the peak conductance of EPSGs and IPSGs, as measured in the soma of one cell, is shown as a histogram of filled and open bars, respectively. These amplitudes were detected at a holding potential of −47 mV. G_{in} without synaptic activity (continuous line) and the synaptic addition to this conductance (dotted line) are shown below the histogram.

DISCUSSION

Neuronal membrane properties are often studied without background synaptic activity, and the integration properties could be different from those seen during network activity. The resistance (R_{in}) and time course of charging (τ_{in}) as measured in soma are important for cell behavior because the somatic compartment is probably the most important integrator for initiation of the sodium spike. These parameters will therefore affect the way synaptic signals are translated into cell discharging. A high value for R_{in} will make PSPs more efficient in terms of amplitude, whereas a slow τ_{in} will prolong the duration of synaptic events. The high values for R_{in} and τ_{in} measured with patch electrodes in slice preparations (3, 4) will, however, give a correct picture of the integration properties during network activity only if the synaptic conductances are small compared with the basal membrane conductance.

Because the neonatal rat spinal cord allows us to combine the study of a locomotor-associated network activity with extensive experimental control, we have been able to show that τ_{in} and R_{in} in neurons that are embedded in an active network increased on average 35%, and rarely more than 100%, when

network activity was blocked by TTX. These changes are considerably more moderate than those suggested for pyramidal cells (5), but are more similar to findings from experiments on visual cortex, which showed 5–20% increases in G_{in} during visual stimulation (21).

Although synaptic activity made moderate changes to τ_{in} and R_{in} over time, the individual postsynaptic conductances (PSGs) at their peak could constitute the major part of G_{in}. In other words, a considerable amount of the synaptic conductance was concentrated over short time intervals, giving a great disparity between a moderate average synaptic conductance (avG_{syn}) and a large conductance of individual PSGs. This is probably even more pronounced in the dendrites, where the higher axial resistance will make the effect of the electrical events more local. Between these extremes (the conductance of individual PSGs and avG_{syn}), there may be periods with a concentration of synaptic conductance. During the locomotor cycle there are usually two halves of the cycle that are each dominated by inhibitory and excitatory synaptic activity. If all the synaptic conductance was concentrated in one cycle half, the values of the synaptic proportion of the membrane conductance would obviously be twice as large as our estimates. The cyclic modulation comes, however, usually on top of a synaptic background activity (22), so the maximal synaptic conductance during one cycle half is probably less than twice the estimated avG_{syn}. These considerations are supported by the lacking or moderate changes in R_{in} between the two cycle halves found in investigations of motoneurons (23, 24).

While there are few assumptions behind the direct measurements of changes in τ_{in} and R_{in} as measured in the soma, it is more problematic to estimate the underlying change in R_m. An increase in R_m will give an increase in both τ_{in} and R_{in}, but not always to similar degrees. The reason why changes in τ_{in} and R_{in} are not necessarily proportional to changes in R_m is that the dendrites have an axial resistance (R_a) that adds to the resistance of the dendritic membrane. The influence of R_a on these parameters increases with long and thin dendrites. We have therefore explored how changes in R_m affect τ_{in} and R_{in} in neurons with different dendritic length through a simulation using the program NEURON (25). The model neuron was constructed with a soma (15 μm) and dendrites as shown in Fig. 4*A*. We used thin secondary and tertiary dendrites (0.5 μm) and R_a in the upper range of what has been reported (300 Ωcm; see, e.g., refs. 26 and 27) because this emphasized the effect of R_a on our estimates. The primary dendrite was 1.5 μm. The diameter of the neonatal rat spinal cord, approximately 1.2 mm, puts a probable limit to the maximal length from soma to the tip of the dendrites. Four cell lengths between 0.15 and 1.2 mm were tested, three of which are shown in Fig. 4 *B* and *C*. For each of these cell lengths we tested values of R_m between 5 and 57 kΩcm^2 because this gave τ_{in} and R_{in} in the range that we had observed in the experiments. The values of R_m were selected so that each new R_m was 50% greater than the previous one.

One obvious effect of long and thin dendrites is that a steady-state voltage induced by a long-lasting current injection into soma has lower amplitude at the tip of the dendrite than in the soma. This attenuation (dendritic tip voltage/soma voltage) of the steady-state voltage amplitude measured in the model neuron is given in Fig. 4*B*. We see that even with relatively high membrane resistance, there may be significant attenuation of the voltage amplitude. This means that areas far away from the soma may contribute less to our estimates for τ_{in} and R_{in}. Therefore, if the conductance changes in the real experiments were not uniform, but localized to the periphery, we would underestimate the changes.

To explore how changes in R_m affected τ_{in} and R_{in} in neurons with different dendritic length, and also to test the limitations of our measuring method, we measured the response to current pulses (20 pA, 300 ms) applied in the soma of the model

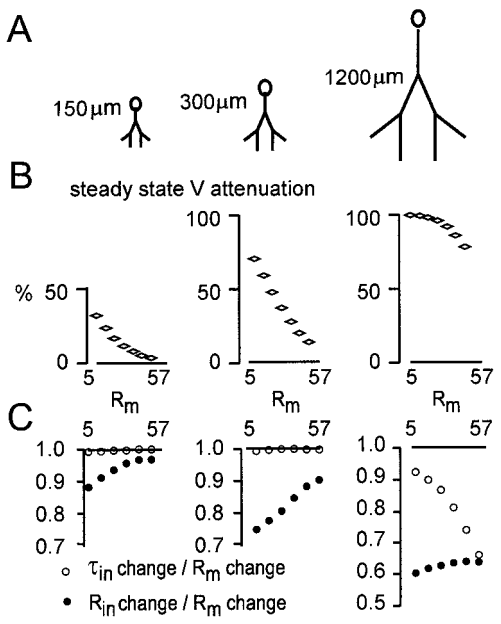

FIG. 4. A model neuron used for simulating changes in τ_{in} and R_{in}. (*A*) Three cell lengths (150, 300, and 1200 μm) are illustrated. For each cell length R_m started at 5 kΩcm^2 and increased 50% of the last value for each run, up to 57 kΩcm^2. This range is given as the *x*-axis in *B* and *C*. (*B*) A steady-state voltage induced by a long-lasting current injection into the soma has lower amplitude at the tip of the dendrite than in the soma. The amplitude at the tip of one dendrite is given as the percent of the somatic amplitude. (*C*) The increases in τ_{in} and R_{in} were compared with a chosen 50% increase in R_m. τ_{in} increased almost proportional to R_m in the cells that were 150 and 300 μm (open circles). When the cells became very long (more than half the diameter of the cord), τ_{in} increased considerably less than R_m, reflecting the limitations of our approach to measure the slowest time constant (see *Discussion*). R_{in} increased generally less than R_m, marked by filled circles, that gives more deviation from unity than τ_{in}.

neuron. We estimated the increases in τ_{in} and R_{in} in response to a chosen 50% increase in R_m between each run [i.e. (τ_{in} with $R_m = 7.5$)/(τ_{in} with $R_m = 5.0$)]. The change in the true membrane time constant (τ_m) would always be proportional to the change in R_m because $\tau_m = R_m$ times a constant capacitance. In Fig. 4*C* we can see that our estimator τ_{in} (open circles) also changed proportionally to the change in R_m when the cells were of moderate size. The ratio between changes in R_m from six different values of R_m between 5 and 57 kΩcm^2 (*x*-axis) and the relative change in τ_{in} is close to 1.0 when the cell is 150 and 300 μm long.

The rightmost plot in Fig. 4 shows that if the cells were very long, in this case the width of the entire cord, the estimation method fails by showing only 60% of the underlying change in R_m, but estimates were within 70% of the true value for an intermediate cell length of 600 μm (not shown). This failure to detect a change in the time constant that was proportional to the change in R_m demonstrates the insufficiency of our measuring method to detect the true τ_m (see *Methods* and ref. 28). The slowest time constant will always be equal to τ_m (20), so by measuring over a later time interval of the charging curve we may, theoretically, have come closer to τ_m. However, when the measurement was delayed, the signal-to-noise ratio became too poor because of the low amplitude of the decaying transient and the large amplitude of the synaptic potentials. As a tradeoff between these factors we chose a time interval (5–25 ms), in the simulation and the real experiments, where the signal-to-noise ratio was the best.

The conclusion is that in the high-resistance cells we recorded from in the spinal cord, the change in τ_{in}, measured in the way we have described, probably reflects at least 70% of the

underlying change in R_m. R_{in} (filled circles) generally changed less than the underlying change in R_m, and is therefore not a good estimator for the change in R_m.

We have not been able to confirm the theory that network activity has very large effects on the membrane resistance (5). This theory was based on simulations of pyramidal cells, which, of course, may be affected more by network activity compared with the neurons from which we have recorded. Many morphological and physiological details, such as the density of synapses, release probabilities, and presynaptic activity, are necessary to know before transferring our findings to other networks. The parameters could also be different in other areas of the central nervous system, in other species, and at different ages. It is also important to be aware that relatively small changes in the average membrane conductance may significantly influence the network function of the neurons (29). Our findings demonstrate, however, that this spinal cord network can operate and produce organized output without a very large and continuous change in passive membrane properties.

We thank Bruce Johnson, Ole Kjaerulff, and Gytis Svirskis for comments on the manuscript. M.R had a European Union Mobility Grant. The work in O.K.'s laboratory is supported by the Danish Medical Research Council and the Novo Foundation.

1. Edwards, F. A., Konnerth, A., Sakmann, B. & Takahashi, T. (1989) *Pflügers Arch.* **414,** 600–612.
2. Blanton, M. G., Lo Turco, J. J. & Kriegstein, A. R. (1989) *J. Neurosci. Methods* **30,** 203–210.
3. Staley, J. K., Otis, T. S. & Mody, I. (1992) *J. Neurophysiol.* **67**, 1346–1358.
4. Spruston, N. & Johnston, D. (1992) *J. Neurophysiol.* **67,** 508–529.
5. Bernander, Ø., Douglas, R. J., Martin, K. A. C. & Koch, C. (1991) *Proc. Natl. Acad. Sci. USA* **88,** 11569–11573.
6. König, P., Engel, A. K. & Singer, W. (1996) *Trends Neurosci.* **19,** 130–137.
7. Smith, J. C. & Feldman, J. L. (1987) *J. Neurosci. Methods* **21,** 321–333.
8. Kudo, N. & Yamada, T. (1987) *Neurosci. Lett.* **75,** 43–48.
9. Cazalets, J. R., Sqalli-Houssaini, Y. & Clarac, F. (1992) *J. Physiol. (London)* **455,** 187–204.
10. Cowley, K. C. & Schmidt, B. J. (1994) *Neurosci. Lett.* **171,** 147–150.
11. Kiehn, O. & Kjaerulff, O. (1996) *J. Neurophysiol.* **75,** 1472–1482.
12. Kiehn, O., Johnson, B. R. & Raastad, M. (1996) *Neurosci.* **75,** 263–273.
13. Kjaerulff, O., Barajon, I. & Kiehn, O. (1994) *J. Physiol. (London)* **478,** 265–273.
14. Carr, P. A., Huang, A., Noga, B. A. & Jordan L. M. (1995) *Brain Res. Bull.* **37.** 213–218.
15. Kjaerulff, O. & Kiehn, O. (1996) *J. Neurosci.* **16,** 5777–5794.
16. Bracci, E., Ballerini, L. & Nistri, A. (1996) *J. Neurosci.* **16,** 7063–7076.
17. Sqalli-Houssaini, Y., Cazalets, J. R. & Clarac, F. (1993) *J. Neurophysiol.* **70,** 803–813.
18. Magistretti, J., Mantegazza, M., Guatteo, E. & Wanke, E. (1996) *Trends Neurosci.* **19,** 530–534.
19. Neher, E. (1995) in *Single Channel Recording*, eds. Sakmann, B. & Neher, E. (Plenum, New York), pp. 147–153.
20. Jack, J. J. B., Noble, D. & Tsien, R. W. (1975) *Electrical Current Flow in Excitable Cells* (Clarendon, Oxford).
21. Berman, N. J., Douglas, R. J., Martin, K. A. & Whitteridge, D. (1991) *J. Physiol. (London)* **440,** 697–722.
22. Raastad, M., Johnson, B. R. & Kiehn, O. (1997 *J. Neurophysiol.* **78**, 1851–1859.
23. Schefchyk, S. J. & Jordan, L. M. (1985) *J. Neurophysiol.* **54,** 1101–1108.
24. Schmidt, B. J., Meyers, D. E. R., Tokuriki, M. & Burke, R. E. (1989) *Exp. Brain Res.* **77,** 57–68.
25. Hines, M. A. (1989) *Int. J. Biomed. Comput.* **24,** 55–68.
26. Major, G., Larkman, A. U., Jonas, P., Sakmann, B. & Jack, J. J. B. (1994) *J. Neurosci.* **14,** 4613–4638.
27. Thurbon, D., Field, A. & Redman, S. (1994) *J. Neurophysiol.* **71,** 1948–1958.
28. de Jongh, H. R. & Kernell, D. (1982) *J. Neurosci. Methods* **6,** 129–138.
29. Hausser, M. & Clark, B. A. (1997) *Neuron* **19,** 665–678.